

The Use of Weather Radar Data: Possibilities, Challenges and Advanced Applications

Maria Silvia Binetti , Claudia Campanale , Carmine Massarelli *  and Vito Felice Uricchio 

Water Research Institute, Italian National Research Council (IRSA-CNR), 70132 Bari, Italy; mariasilvia.binetti@ba.irsa.cnr.it (M.S.B.); claudia.campanale@ba.irsa.cnr.it (C.C.); vito.uricchio@ba.irsa.cnr.it (V.F.U.)

* Correspondence: carmine.massarelli@ba.irsa.cnr.it

Abstract: The climate in recent decades has aroused interest in the scientific community, prompting us to analyse the mechanisms that regulate it, to understand the climate change responsible for an increase in extreme phenomena. Consequently, the increase in hydrogeological instability in the Italian territory has led to an in-depth study of atmospheric parameters to understand the variations of the atmospheric system. One tool capable of detecting such variations is the weather radar. The weather radar data available in the area provided by the National Radar Network of the Department of Civil Protection allow the evaluation of variations on a national scale for hydro-meteorological-climatic monitoring as well as the disasters that have occurred. Using open-source programming software, the servers can be queried and data retrieved from a source to perform processing for specific purposes through data extraction techniques.

Keywords: weather radar; extreme events; rainfall; flash floods; landslide; disaster management; open-source software; python



Citation: Binetti, M.S.; Campanale, C.; Massarelli, C.; Uricchio, V.F. The Use of Weather Radar Data: Possibilities, Challenges and Advanced Applications. *Earth* **2022**, *3*, 157–171. <https://doi.org/10.3390/earth3010012>

Academic Editor: Charles Jones

Received: 30 November 2021

Accepted: 31 January 2022

Published: 3 February 2022

Publisher's Note: MDPI stays neutral with regard to jurisdictional claims in published maps and institutional affiliations.



Copyright: © 2022 by the authors. Licensee MDPI, Basel, Switzerland. This article is an open access article distributed under the terms and conditions of the Creative Commons Attribution (CC BY) license (<https://creativecommons.org/licenses/by/4.0/>).

1. Introduction

Climate is the synthesis statistic of atmospheric parameters (temperature, rain, moisture, pressure, wind) which involve an area over a long time [1]. In recent decades, the climate has aroused interest in the scientific community pushing us to analyze the mechanisms that regulate climate change. In this respect, the Glossary of Meteorology [2] provides the following definitions for climate change: any systematic change in the long-term statistics of climate elements (such as temperature, pressure, or winds) sustained over several decades or longer. Climate change is considered responsible for extreme weather events (tornadoes, high winds, hailstorms, flash floods) due to natural external or anthropogenic forcing [3]. Severe convective weather events trigger or have the potential to trigger flash floods, landslides and potential hazards. The damages associated with extreme weather events are relevant in terms of human and social costs; between 1980 and 2019, the European Environment Agency (EAA) member countries suffered economic losses totaling an estimated USD 500 billion [4]. In Italy, the situation is made worse by small catchments along coastlines and by the Alps and Apennines Mountain chains.

This paper proposes an overview of radar applications, potential uses and a system for the extraction of elaborated weather radar data. Data are based on open-source software, useful for producing new thematic maps, to reconstruct historical data related to a particular event. The project provides access to information to allow risk assessment. This project is addressed to administrators, institutional users and citizens.

This paper is organised as follow:

- Section 1 provides a brief introduction to the theoretical background of Weather radar;
- Section 2 shows the potential use of weather radar resources in various applications such as military, nautical, aviation, marine, meteorology, biology and weather surveillance;

- Section 3 describes the hydrologic applications of weather radar with a focus on catastrophic impacts caused by floods;
- Section 4 summarizes the recent advanced worldwide applications and report the result of the Italian case history and, in detail, the Puglia Region case study with a brief discussion;
- Section 5 reports conclusions and opportunities for future work.

Theoretical Background

The history of Weather Radar (abbreviation of RAdio Detecting And Ranging) begins during World War II, when military radar operators noticed extraneous echoes showing up on their display. David Atlas was one of the pioneers of radar meteorology, along with John Stewart Marshall, Walter Palmer and Richard Doviak [5]. After the second world war, John Stewart Marshall and Walter Palmer investigated Z-R relationships in the Stormy Weather Group. Furthermore, Richard Doviak was the father of Doppler radar at the National Oceanic and Atmospheric Administration (NOAA) for storm forecasting. These are just some of the milestones in the origins of weather radar.

Weather radars send pulses of electromagnetic energy into the atmosphere, a microsecond of long microwave radiation to identify the presence of hydrometeors [6]. Hydrometeors from the Greek *hýdōr-metēōros*, which means literally “water that is high in the sky” represent all phenomena of condensation and precipitation of atmospheric humidity in liquid or solid particles. When the pulses strike an object such as rain, hail, or snow, Rayleigh scattering occurs and part of the energy is reflected back to the radar receiver (Figure 1) [5]. Rayleigh scattering takes place when the wavelengths are greater than the diameters of the hydrometeor particles. Different wavelengths identify particles of different sizes. Rayleigh scattering starts to become invalid when the hydrometeor diameters are large (e.g., 2–3 cm) compared to the wavelength of the X-band. The X-band has the shortest wavelength compared to the S and C bands.

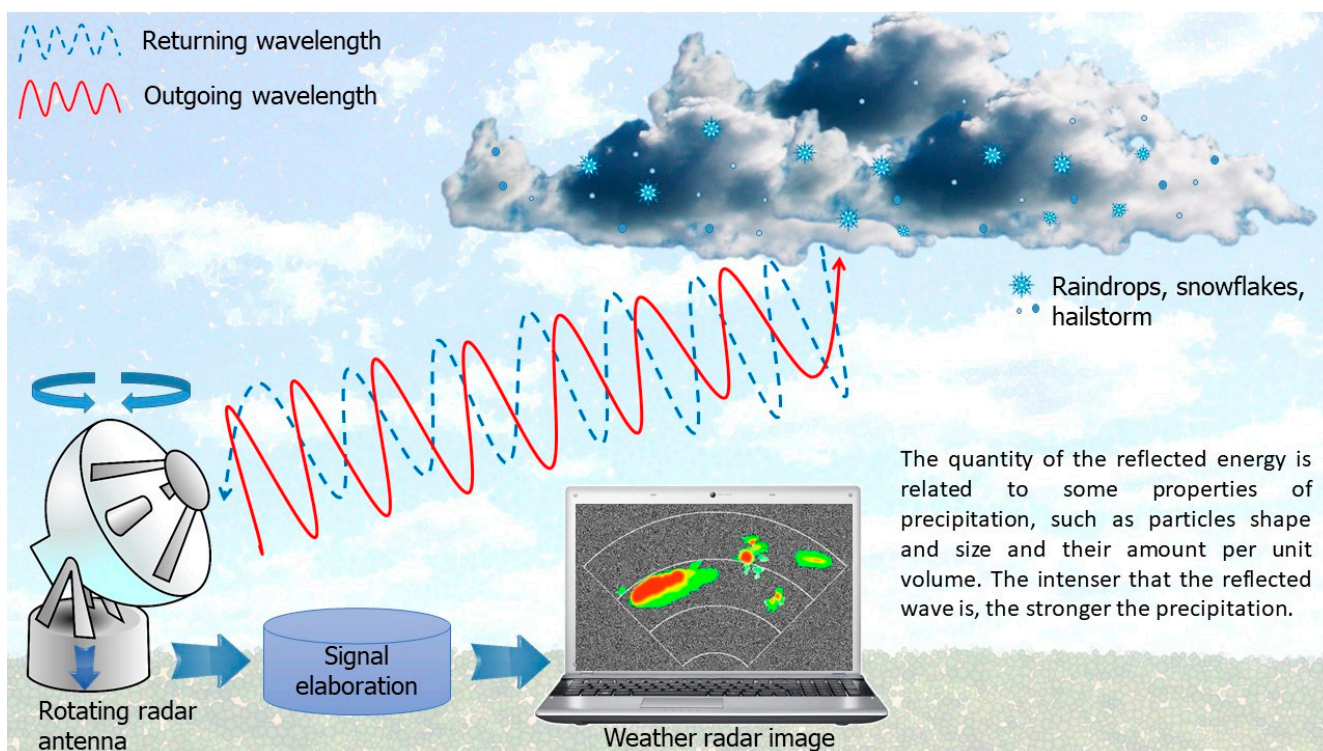


Figure 1. Weather radar principle of function. Weather radar image reworked from source [7].

Weather radar works in three different frequency bands: S, C and X. S-band radar has a longer wavelength (8–15 cm) and can provide rain detection up to 300 km. C-band radar is medium-range (4–8 cm) and measures up to 200 km, and finally, the X-band radar is the smallest wavelength (2.5–4 cm). These waves are well-suited for measuring up to a range of 50 km [8]. Further, L-band radar (15–30 cm), with a frequency of 1–2 GHz, is used for clear air turbulence studies, and K-band radar (0.75–1.2 or 1.7–2.5 cm), with a frequency of 27–40 and 12–18 GHz, is similar to the X-band, but more sensitive when compared to them. For example, in heavy rain, due to radar signal attenuation in the X-Band, the reflectivity information can be completely hidden from radar scans [9]. This does not happen for K-Bands.

Weather radars have five components: transmitter, antenna, radar processor, receiver, display system. The transmitter generates electromagnetic pulses and the antenna sends pulses into the atmosphere and receives the reflected pulses. The antenna dish can rotate 360 degrees horizontally and scan the atmosphere volume using different elevation angles. The radar processor analyses the received data, and the receiver identifies the signal and amplifies the weak signals received. Finally, the data system displays the radar data to their viewers.

The precipitation estimate can be driven from different measurement techniques, such as weather radar networks, rain gauge networks and meteorological satellites.

The weather radar equation is founded on the basic principles of radar, on the power of transmission, propagation and reception of echo signals:

$$P_r = \frac{P_t \cdot G^2 \cdot \lambda^2 \cdot \sigma}{(4\pi)^3 \cdot r^4} \quad (1)$$

where P_r is the received power, P_t is the transmitted power, G is the antenna gain, σ is the radar cross-section and λ is the transmitter's wavelength [9]. The weather radar does not measure rainfall directly but instead uses an algorithm to estimate rainfall from radar observation [10,11]. The radar calculates rainfall intensities, R (mm h^{-1}), from the observed radar reflectivity, Z ($\text{mm}^6 \text{m}^{-3}$), in single-polarized radar [12]. The rainfall intensity and reflectivity are related by a power law [13]. The coefficient of the power law relationship is required to transform reflectivity to rainfall rate [14]. Dual-polarized radar produces both horizontal and vertical electromagnetic waves to detect the shapes, size, density and distribution of water droplets in the atmosphere [15].

The radar reflectivity Z product displays echo intensity measured in decibels (dBZ). Depending on the software system or user preference, the colors display the different echo intensities, from very weak to very strong hydrometeors. For example, the green–light-blue is related to light rain precipitation when the dBZ value touches 20. The yellow (approximately 35 dBZ value) shows moderate precipitation, while red (approximately 50 dBZ value) is for heavy precipitation. The higher radar reflectivity is related to hailstones mixed in with the liquid hydrometeors (approximately 65 dBZ value).

The rain gauge network measures the accumulated rainfall as a function of time. This technique uses a point measurement with a temporal resolution of 1 min–1 h. The instruments count drop measure differently to disdrometers, which measure the statistical distribution of drop size [14].

Finally, meteorological satellites for rainfall estimation were developed to strengthen hydrological models and weather forecasting [16]. Rainfall estimates from the radar can also be combined with estimates from meteorological satellites, potentially strengthening the reliability of hydrological models and weather forecasts.

There are numerous sources of errors that affect the weather radar measurement. The errors are due to hardware error, radar beam geometry, scan strategy, the distance from the radar site, echoes from the non-meteorological target, orographic obstacles, attenuation signal and anomalous propagation of the radar beam [8,17,18]. It is important to be familiar with the errors of the radar measurement and the processing complexity.

2. Potential Use of Weather Radar Resources

Radar is used in various applications, such as military, nautical, aviation, marine, meteorology, biology and weather surveillance. Weather radars are essentially employed for measurement and forecasting atmospheric phenomena.

The drastic increase of extreme weather events has led to increased frequency and severity of flood events. Hus et al. [19] developed an automatically combined ground weather radar with images in real-time for flood monitoring. Closed-circuit television systems were combined with automatically combined ground weather radar, providing information regarding the water level in flood monitoring. This system allows one to make a quick evacuation decision to reduce the adverse effect. Rapant et al. [20] presented a method with a different technique to obtain a dynamic pluvial flash flooding hazard forecast. This approach uses weather radar data to carry information on the current precipitation distribution, watershed and drainage network. In more detail, the 2D weather radar data are transformed into 1D signals related to the section of watercourses. If the system detects danger, it sends a possible warning of flash flooding to neighbouring municipalities. The experimental result showed a substantial reduction in false alarms against imminent flash floods, including the saturation indicator.

Another application of weather radar is wildfire monitoring and filling in the knowledge gaps regarding dangerous fire conditions. Wildfires constitute considerable natural hazards, and Doppler radar can be used to identify the fire behaviour of wildfire plumes [21].

Maki et al. [22] analyse 3D weather radar data from volcanic eruption clouds to understand the ash-fall transportation. It is possible to construct a radar reflectivity microphysical model to quantify the eruption regimes [23]. Building off previous experimental observations, it is possible to achieve the classification of eruption regime and volcanic ash category and estimate ash concentration.

Voormansik et al. [24] presented a method to detect thunderstorm hail and lightning with C-band dual-polarization Doppler radar. These convective storms, associated with lightning and hail, cause financial losses and significant damage to infrastructure. The radar lightning estimation identifies which cells are rapidly growing and approaching the measures likely to produce lightning in the foreseeable future. The study is based on four years of the summer periods in Estonia; it was found that 33.9% of the identified cells produced lightning and 25.9% produced hail.

Weather radar can be used in biology to study bird migration at temporal and spatial scales. The detailed information on the areal movements of an organism can be explored to create interpreting regional-scale migration patterns and information in the landscape and aerial environment [25]. Polarimetric radar observation is used for bird detection. Furthermore, recent studies have been conducted using weather radars to explore the harmful influence of artificial light on migratory bird populations [26]. Using multi-year weather radar measurement, it has been shown that birds are attracted to artificial light while in flight, and this inhibits habitat selection. The choice of high-quality stopover habitat is crucial for the conservation of bird populations. Another study evaluated the spatial and temporal variation in nocturnal migration patterns that are affected by winds. This first continental-scale study used 70 weather radar stations in Europe for investigating the ecosystem consequences of large-scale bird movements [27]. Several studies report the impressive decline of bird population that defined the global biodiversity crisis [28].

Current weather radar literature research has investigated the offshore wind fluctuations for optimizing the administration of wind farms in real-time. Trombe et al. [29] present an automated decision-support system based on the collection of meteorological observations at high spatio-temporal resolutions to provide relevant inputs to prediction systems. Also of relevance is the interference of echoes from the wind farm to weather radar [30].

The use of weather radar also concerns human health. Using machine learning methods and Next Generation Weather Radar data, it is possible to estimate daily pollen

over a $300 \text{ km} \times 300 \text{ km}$ region at a resolution of $0.5 \text{ km} \times 0.5 \text{ km}$ [31]. The models are developed using radar measurements of reflectivity, direction and speed of the wind, line of sight Doppler velocity and spectral width at the lowest two elevations to estimate the daily pollen dispersal. The study results provide pollen alerts and predict allergic pollen of different species.

Recent weather radar literature has investigated the Radar Simulator, which can reproduce realistic weather radar measurement [32–34]. The simulation starts from a known meteorological scenario to build processing algorithms.

The increasing use of weather radar generates a large amount of data transmission and storage. Zeng et al. [35] present a weather radar lossless compression approach called spatial and temporal prediction compression (STPC).

Regarding interference in weather radar, the growth of wireless telecommunication systems represents the primary concern with regards to guaranteeing radar data quality. The electromagnetic interference negatively affects the quantitative precipitation estimation and can lead to a biased hydrometeor classification [36]. Oh et al. [37] proposed a clutter elimination algorithm for the non-precipitation echo of radar data, such as anomalous propagation and interference, biological target and sea clutter.

Concerning airborne weather radar, the literature is extensive. Airborne weather radar detect potential weather hazards during flight. Li et al. [34] introduce a microphysics-based simulator applied in different weather scenarios to address the theoretical basis and uncertainties of hydrometeor scattering. Nepal et al. [38] present a radar implementation on a low-cost weather radar platform for multi-mission applications. Nekrasov et al. [39] developed a conceptual approach for measuring near-surface wind vectors with airborne weather radar to predict the future sea surface conditions and weather patterns.

3. Hydrologic Applications of Weather Radar

Surface precipitation measurements are extremely important in hydrology, climatology and meteorology studies. These data can be improved by using weather radar and conventional rain and snow gauges.

Recent advances in digital radar data management make it possible to provide high-resolution quantitative precipitation information (QPI) for a wide range of hydrological applications [40]. With the progress of Geographical Information System (GIS) technology, radar-based quantitative precipitation estimates (QPE) have enabled routine high-resolution hydrologic modeling worldwide [41]. Recent progress and changes in weather radar hydrologic applications make its use a crucial tool for water resource management. The main topics of growth concerning weather radar applied to hydrology related to: (i) radar QPE [42–46], (ii) multi-radar and multi-sensor precipitation analysis [47–49], (iii) hydrologic modelling [50–52], (iv) urban hydrologic and hydraulic applications [48,53–56], (v) precipitation frequency analysis [57,58], (vi) hydrometeorological process studies [59,60], (vii) precipitation nowcasting, forecasting [61], (viii) hydrometeorological applications [62].

Floods Forecasting

Catastrophic impacts caused by floods worldwide will tend to grow due to more frequent climate changes in the next few years [63]. A flood is an excess of water that inundates usually dry land, with tragic effects. The factors responsible for flooding include the greenhouse effect, seismic and neotectonics activities, excessive development, soil erosion, damming of rivers, deforestation, riverbed aggradation, subsidence and compaction of sediments, inadequate sediment accumulation and local relative sea-level rise [64]. The negative impact of flooding includes economic damage to structures, roadways and bridges, and especially life loss [65–67].

An essential component of flood management is implementing and improving flood forecasting and warning systems.

Over the past years, institutions have adopted different data collection systems for supporting flood management, including rainfall gauges, hydrological stations, humidity sensors, and weather data. Unlike in situ sensors capable of monitoring only a limited region, weather radar is remote sensing-based equipment that measures the volume of rainfall over an entire area instead of measuring a single point.

Recently, several countries have investigated using weather radar precipitation to improve situation awareness in a disaster and early warnings (e.g., floods). In a case study carried out in São Paulo, Brazil, in the period 2017–2018, crowdsensing and weather radar data together helped generate high-quality information at more satisfying spatial and temporal resolutions to improve the decision-making related to weather-related disaster events. Rainfall data provided by two weather radars located in the city were used to validate flooded areas identified by volunteered information. Moreover, a clustering approach identified those flooded areas, which may support more informative decisions in flood management.

Based on the soil saturation, the physical-geographical characteristics of an area and QPEs and forecasts (QPFs) is possible to calculate a Flash Flood Indicator (FFI). This system is used at the Czech Hydrometeorological Institute to evaluate the risk of flash floods resulting from torrential rainfall events over the whole Czech Republic. To improve the accuracy of flash flood forecasting, accurate calculations of QPEs and QPFs are required [68].

Radar data were also used in 2021 to test a new method in the Czech Republic to forecast the flash flooding hazard usually occurring in very small, typically ungauged, watersheds using raw weather radar data and watercourse network. The developed method can provide a map of the flash flooding hazard distribution on the watercourse sections. This result allows an evaluation of the identified hazard and a risk estimation for inhabitants of the area, with a system of alerts for municipalities [20].

In Taiwan, taking advantage of a dense network of surveillance cameras installed in the city, an automatic ground weather radar (ARMT) and a closed-circuit television system were combined to develop images for real-time flood monitoring. The system integrates real-time ground radar echo images and automatically estimates a rainfall hotspot according to the cloud intensity, providing real-time warning information. The ARMT showed reliability between 83 and 92% using historical data input, while with real-time data, reliability slightly decreased from 79 to 93% [19].

4. Overview of Recent Advanced Worldwide Applications

There are many weather radar applications in multiple areas. Table 1 reports the most significant studies, with their reference, for applications that we consider most representative, with a summary regarding the principal aims. The applications are divided into two main categories: natural disasters (flood events, wildfires, volcanic ash) and the enhancement of ecosystem services (airborne, urban hydrology, bird migration), which indicate the many advantages to humans furnished by the natural environment and from healthy ecosystems, as popularized in the Millennium Ecosystem Assessment [69].

Table 1. Recent advanced worldwide applications.

Application		Principal Aim Application	Year of Publication	Reference
Natural disasters	Flood events	Substantial reduction in false alarms	2021	[20]
	Volcanic ash	Understanding of volcanic eruption column dynamics and horizontal ash-fall transportation with three-dimensional analyses	2021	[22]
	Wildfires	A better understanding of fire behaviour and fire atmosphere interaction	2019	[21]
	Thunderstorm hail and lightning	Reduced financial losses and significant damage to infrastructure products by thunderstorm hail and lightning	2017	[24]
Enhancement of ecosystem services	Bird migration	Detailed information on bird movements in the landscape and aerial environment	2020	[25]
	Wind farms	Detecting interference from wind farm echoes	2019	[30]
	Pollen concentration	Providing pollen alerts and predicting allergic pollen of different species	2019	[31]
	Urban hydrology	Improve the applicability of radar and rain gauge rainfall estimates	2019	[55]
	Airborne	Radar implementation low-cost for multi-mission applications	2017	[38]

4.1. Italian Case Studies

The Italian Civil Protection Department is designed to monitor weather-hydrological and volcanic ash fallout. The Department has the fundamental role of gathering and coordinating the national resources necessary and ensuring assistance to the population in case of emergency.

The Italian national weather radar network is coordinated by the Civil Protection Department (DPC), in collaboration with the Air Traffic Control service (ENAV), the Weather Service of the Air Force (CNMCA), regional authorities and research centers. The Italian radar network includes both C-band radars and five dual-polarized X-band radars, deployed throughout the country [70]. The Civil Protection Department provides a platform called Radar-DPC [71] that allows seeing both ongoing phenomena and those of the previous six days on a national scale. This platform provides basic products, previously processed data from ground stations networks, satellite and lightning [72]. We focused on Vertical Maximum Intensity (VMI), which represents the maximum reflectivity value present in the vertical column above each point. The VMI can be used for general monitoring, as it allows one to distinguish very well the areas in which significant phenomena are underway and to classify them according to their type (fronts, convection systems, etc.). The reflectivity dBZ is a quantity directly related to the cloud's density, and therefore to the water content. Reflectivity values higher than 10 dBZ usually (but not necessarily) indicate the presence of precipitation on the ground (values lower are typically not displayed to avoid disturbances and/or residues of unwanted clutter, increasing the data quality threshold). Reflectivity values above 40 dBZ are considered very intense, and when value of 45 dBZ are reached and exceeded, there is a high probability of extreme phenomena dangerous for people, animals or things, and these values typically indicate the presence of convective storms with high rainfall rates.

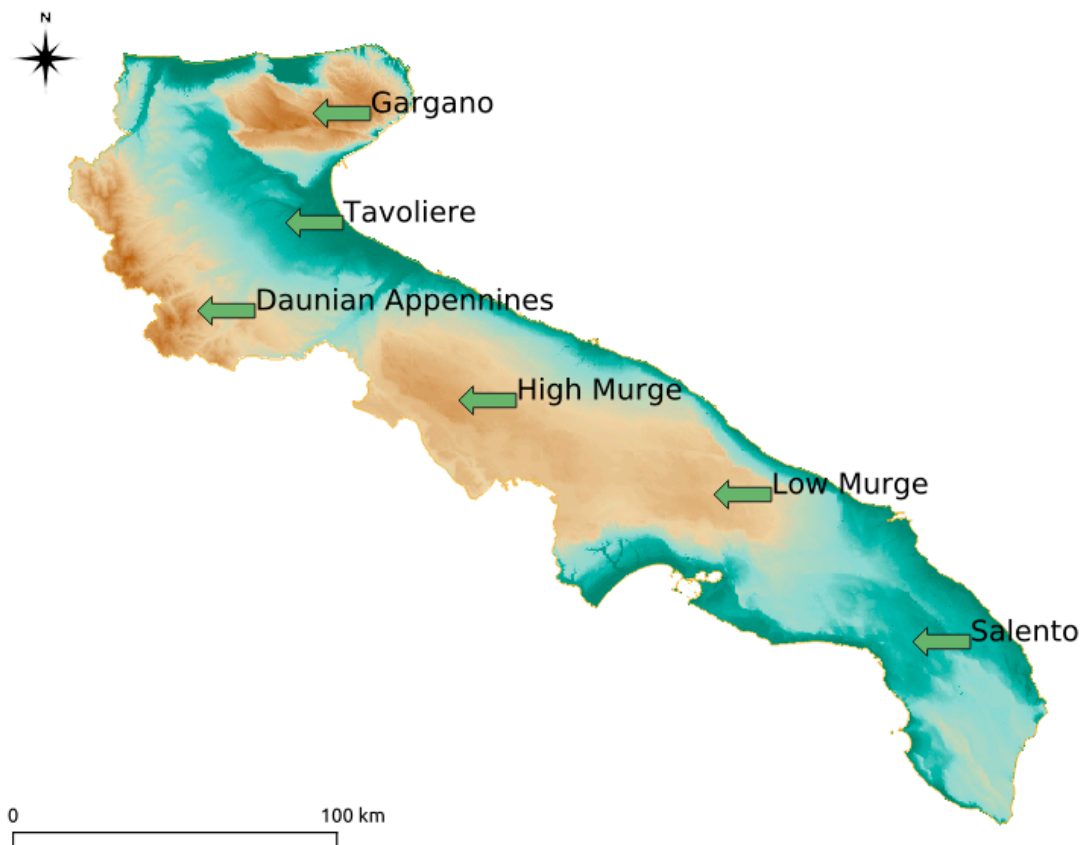
4.2. The Puglia Region Case Study

The Puglia region is located in southern Italy and shows landform depending on structural and geolithological factors. The prevailing morphologic characteristic of the Apulian region is the presence of plains and hills with highly diversified climatic conditions [73]. It is possible to discern the area in five main physiographic areas: Daunian Appennines, *Gargano*, *Tavoliere*, high and low *Murge* and *Salento*. The region is segmented by a NW-SE trending normal fault, divided into three structural blocks of Mesozoic limestone with different degrees of uplift: *Gargano*, *Murge* and *Salento*. Daunian Appennines, the eastern boundary of the southern Appenninic chain, is characterized by hilly landscapes, with the highest peak being approximately 1150 m. The *Tavoliere*, the northern part of the Bradanic Trough domain, is the wildest alluvial plain in south Italy (Figure 2).

In recent years, there have been more and more frequent phenomena of soil instability related to the evolution of the slopes, the collapses along the high coast and the sinking of underground cavities as well as floods for which, given the heterogeneity of the territory, it is always difficult to correctly identify the areas involved as it is necessary to process the data further. So, considering the particular characteristics of the territory and above all its heterogeneity, in order to insert a further phase of data processing that could also include these geomorphological aspects of the territory, a system for data extraction and use of weather data in real-time has been implemented, followed by a specific processing workflow. This application has been tested at a regional scale. The technique, called data extraction, refers to the process, put into practice by a user, of extracting and retrieving data from a data source to perform further processing or storage.



(a)



(b)

Figure 2. (a) Administrative limits of the Puglia region (Base map from Bing Maps). (b) Geographical subdivisions based on the morphology of the territory of the Puglia region (Base map from SIT Puglia [74]).

The created real-time radar weather data system extracts the weather-climatic data from DPC. Its data structures are implemented through relational databases and are based on a complex system architecture [75]; the services [76] are provided through an open-source server for sharing geospatial data designed for interoperability [77]. These services are provided according to the standards [78].

Consultation of the DPC platform [71] takes place through interactive maps and allows access to weather-radar products compatible with international standards to exchange geo-related data.

The spread of web databases has made numerous data accessible to users [79]. As mentioned, the DPC radar platform allows the visualization of radar weather data over the previous seven days; on this assumption, a specific data extraction procedure has been implemented based on the open-source scripting language python [80], as shown below. Python was chosen because it is considered very robust and highly versatile and has a consistent number of python bindings [81], which are packages and extensions tools for programming and manipulating the Geospatial Data Abstraction Library (GDAL) [82].

First of all, it is important to be aware of the territory extension to extrapolate the data, the resolution with which these are provided and, consequently, the coordinates of the bounding box based on information [83].

The data extraction system has been implemented through python scripts based mainly on the *ogr*, *gdal*, *pyproj*, *NumPy* and *PIL* libraries and allows the geo-referencing of the information, which can be viewed on the radar platform available to the user.

Below we report the rules used for data extraction and georeferencing in pseudocode format; this is a way of expressing an algorithm without conforming to specific syntax rules and is an efficient way to communicate ideas and concepts (note that indentation represents nested code). The purpose of inserting this pseudocode is to make people understand the operating principles of the extraction technique implemented in order to be able to replicate it.

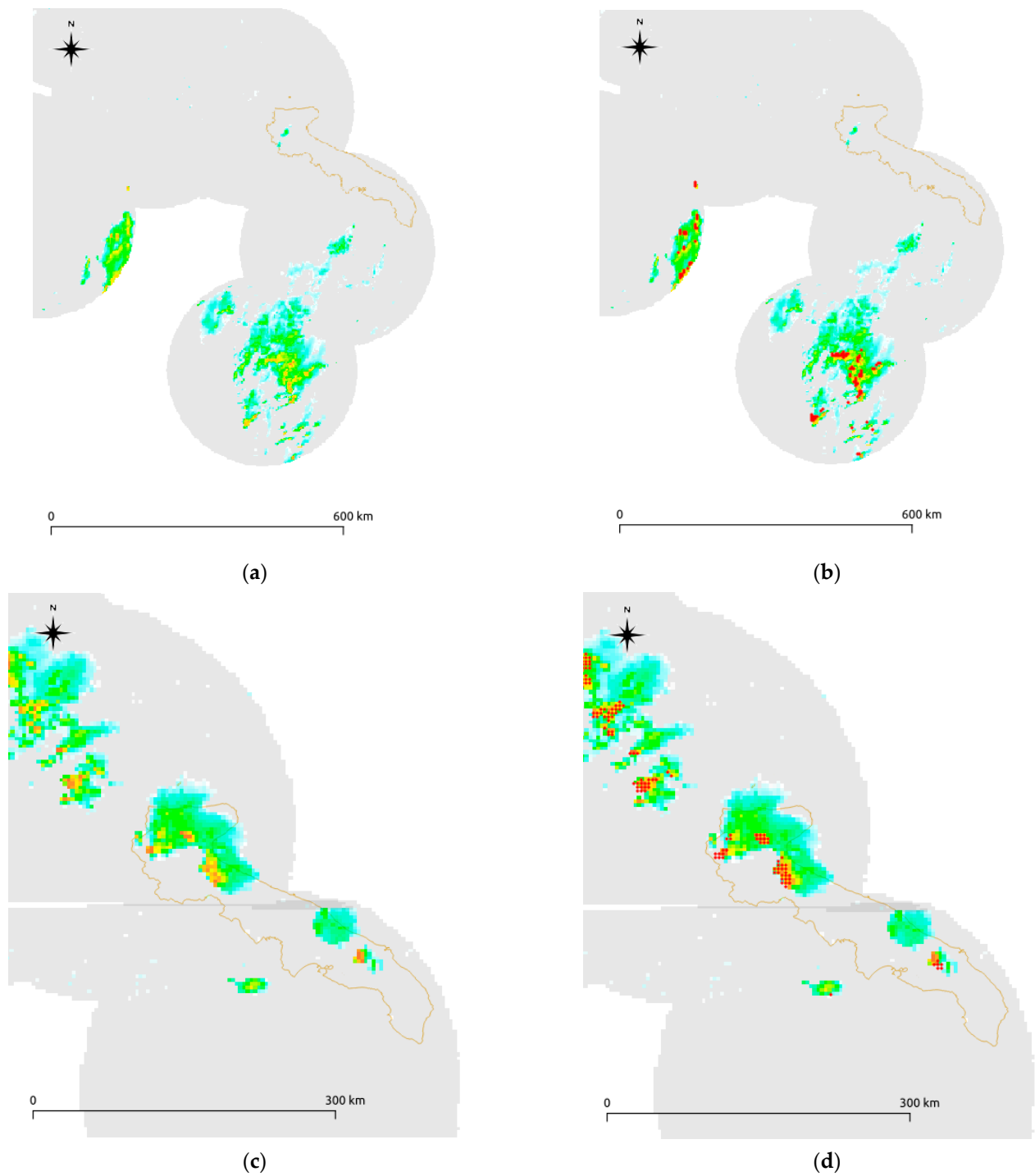
```

START
defining bounding box
defining time of the query
executing query via urllib.urlretrieve method
saving the tiles provided as the response from DPC servers
load the image tiles in the memory
transform the images into NumPy array
for each X Y dimension of the NumPy array do this:
  if parameters of X and value of Y is more than 250 for component
  Red and equal to 0 for the components Green and Blue of the
  colours:
    save these coordinates in another NumPy array
open this second array of coordinates
for each couple of coordinates memorised and considering the X and
Y coordinates of the bounding box:
  add a line to a file with attributes coordinate_X and
coordinate_Y
save the file
END
(An array is a grid of values and it contains information about the
raw data, how to locate an element and how to interpret an element.
It has a grid of elements that can be indexed in various ways.)

```

The DPC servers are queried by executing the script, the data of interest selected and the radar weather data tiles for the area of interest saved in the PC. The areas with powerful phenomena in progress are then selected, processed and classified as fronts or convection systems, and their coordinates are saved.

Below are the reported results of *n*; two tests were performed on the whole Puglia territory. It is possible to view the perimeter of the Puglia Region, the coverage map of the radar services provided with the VMI parameter and the result of the script execution. The red dots represent points of a shapefile imported into a Geographical Information System (GIS) of very heavy rain cores present at that time (Figure 3).



Legend

Colour bar related to the intensity of the phenomena in progress from DPC.



● Vertical Maximum Intensity Points obtained after executing the script.

— Administrative limits of Puglia Region.

Figure 3. Example of two tests carried out: (a) and (c) are data from DPC servers, respectively, on 4 July 2020 and at 21:00 and 14 October 2021 at 17:00, (b) and (d) are the same data with the point obtained after running the script and imported into a GIS system.

Figure 3 shows how the data extraction technique outputs a reliable result. Other tests have been carried out, but the results have always only been satisfactory. The points with a red circle (on the right of the figures), obtained from data on the left of the figure, have been imported into a GIS system and superimposed on the official data of the DPC. Therefore, we can assert that the extraction technique works well as we can now use the data provided according to our needs. Moreover, this can be done every time the DPC data is updated, i.e., every 15 min.

The use of the processed data, made possible by implementing this ICT tool through the scripting language in python, allows any user to query the databases and obtain solid rainfall values related to a specific territory point in a given moment. Following the query, the result could also be provided in the form of a summary report or information sheet containing a series of useful information relating to the calculation and validation process already carried out by the DPC, which is very useful for understanding the phenomena in progress and those that have previously taken place, and also for insurance purposes. Pursuing this goal, where the areas of interest and the reasons require it, we could apply geostatistical techniques and algorithms to obtain more precise results according to the peculiarities of the considered area. This result could also be pursued by integrating the data with other available data sources, such as the weather stations of the Regional Agrometeorological Service (ARIF) [84] and those provided by the Regional Agency for the Prevention and Protection of the Environment (ARPA) [85]. Regarding this, it seems relevant to us to implement an Inverse Distance Weighted (IDW) based spatialization algorithm contemplating other factors such as the altitudes, the distance from the sea and rivers (the five largest in Puglia) to obtain measurements more accurate by weighing the recorded values with the mutual distances.

The IDW algorithm represents a deterministic spatial interpolation method (it produces the same results if the input data are the same) proposed by Shepard [86]. It is one of the more popular methods used by hydrologists and earth scientists, it is easy to implement, and most specialized software integrates it among the basic options. It is applied to estimate unknown values based on known values, assuming closer values are more related than further values. It uses only distance to make estimates. For this reason, we believe it necessary to implement it by integrating the calculating of the weighted values of other variables.

Finally, working exclusively with open-source software, the goal is to develop interoperability services and tools between databases. This makes the maximum diffusion and use of high value-added services for the Public Administration possible, increasing the potential of the interoperability standards that can be implemented, for which the Italian Agency has recently adopted the Guidelines [87].

5. Conclusions and Future Challenges

This study proposes an overview of possibilities, challenges and advanced applications in weather radar. Weather radar measurements have enormous prospective in various applications, in particular hydrological ones. As a result of straightforward reworking, the weather radar data of the Department of Civil Protection can be used and enhanced in the different regional territories for different purposes. The approach identified and described in this report allows the extraction of weather radar data. These data evolve into information and then into knowledge. This is easily divulged for the provision of a series of predictive services, emergency management and the assessment of damage resulting from extreme events. In addition, python proves to be a versatile and powerful tool for managing data with a strong space-time connotation. Because of this, it was possible to develop a new ICT tool that was able to use information already available but in a different way from how it is currently used, for example, for insurance purposes. This can ensure fair rewards for citizens affected by extreme events and identify the illegal conduct of undue claims.

Author Contributions: Conceptualization, M.S.B., C.M. and C.C.; methodology, M.S.B. and C.M.; software, C.M.; validation, M.S.B., C.M. and C.C.; formal analysis, M.S.B., C.M. and C.C.; investigation, M.S.B.; resources, C.M. and V.F.U.; data curation, M.S.B. and C.C.; writing—original draft preparation, M.S.B. and C.C.; writing—review and editing, M.S.B., C.M. and C.C.; visualization, M.S.B., C.M. and C.C.; supervision, C.M.; project administration, V.F.U.; funding acquisition, V.F.U. All authors have read and agreed to the published version of the manuscript.

Funding: This research was funded by Omninet Group.

Institutional Review Board Statement: Not applicable.

Informed Consent Statement: Informed consent was obtained from all subjects involved in the study.

Acknowledgments: We thank ©2021 Omnitech, S.r.l., Omninet Group for helpful discussions in this study.

Conflicts of Interest: The authors declare no conflict of interest. The funders had no role in the design of the study; in the collection, analyses, or interpretation of data; in the writing of the manuscript; or in the decision to publish the results.

References

- Bonci, L.; Malcevschi, S.; Belvisi, M.; Piccini, C.; D’Ambrogi, S.; Ercole, S.; Giovagnoli, M.C.; Franchi, G.; Morelli, E.; Parente, S. *Dynamic Glossary for the Environment and Landscape*; Manuals and Guidelines 78/2012; ISPRA: Rome, Italy, 2012.
- Mahoney, J.R. AMS 2000: A Strategic Review. *Bull. Am. Meteorol. Soc.* **1990**, *71*, 504–506. [CrossRef]
- Mapes, J.A.; Johnson, R.H.; Mapes, B.E. Mesoscale Processes and Severe Convective Weather. In *Severe Convective Storms*; American Meteorological Society: Boston, MA, USA, 2001; pp. 71–122. [CrossRef]
- Economic Losses from Climate-Related Extremes in Europe. Available online: <https://www.eea.europa.eu/ims/economic-losses-from-climate-related> (accessed on 19 December 2021).
- Bringi, V.; Zrnic, D. Polarization Weather Radar Development from 1970–1995: Personal Reflections. *Atmosphere* **2019**, *10*, 714. [CrossRef]
- Battan, L.J. *Radar Observation of the Atmosphere*; University of Chicago Press: Chicago, IL, USA, 1981.
- File: Weather-Radar-Blind-Zone.png—Wikimedia Commons. Available online: <https://commons.wikimedia.org/wiki/File:Weather-radar-blind-zone.png> (accessed on 8 January 2022).
- Sokol, Z.; Szturc, J.; Orellana-Alvear, J.; Popová, J.; Jurczyk, A.; Céleri, R. The Role of Weather Radar in Rainfall Estimation and Its Application in Meteorological and Hydrological Modelling—A Review. *Remote Sens.* **2021**, *13*, 351. [CrossRef]
- Rahimi, A.R.; Holt, A.R.; Upton, G.J.G.; Krämer, S.; Redder, A.; Verworn, H.R. Attenuation Calibration of an X-Band Weather Radar Using a Microwave Link. *J. Atmos. Ocean. Technol.* **2006**, *23*, 395–405. [CrossRef]
- Bringi, V.N.; Chandrasekar, V. *Polarimetric Doppler Weather Radar: Principles and Applications*; Cambridge University Press: Cambridge, UK, 2001; p. 636.
- Anagnostou, E.N.; Krajewski, W.F.; Smith, J. Uncertainty quantification of mean-areal radar-rainfall estimates—Web of Science Core Collection. *J. Atmos. Ocean. Technol.* **1999**, *16*, 206–215. Available online: <https://biblioproxy.cnr.it:3009/wos/woscc/full-record/WOS:000078683100003> (accessed on 24 November 2021). [CrossRef]
- Mahmood, D.A. Estimation of Dual Polarization Weather Radar Variables. *Al-Mustansiriyah J. Sci.* **2018**, *28*, 1. [CrossRef]
- Morin, E.; Krajewski, W.F.; Goodrich, D.C.; Gao, X.; Sorooshian, S. Estimating Rainfall Intensities from Weather Radar Data: The Scale-Dependency Problem—Web of Science Core Collection. 2003. Available online: <https://biblioproxy.cnr.it:3009/wos/woscc/full-record/WOS:000185945200002> (accessed on 23 November 2021).
- Michaelides, S.; Levizzani, V.; Anagnostou, E.; Bauer, P.; Kasparis, T.; Lane, J.E. Precipitation: Measurement, remote sensing, climatology and modeling. *Atmos. Res.* **2009**, *94*, 512–533. [CrossRef]
- Ku, J.M.; Na, W.; Yoo, C. Parameter estimation of a dual-pol radar rain rate estimator with truncated paired data. *Water Supply* **2020**, *20*, 2616–2629. [CrossRef]
- Levizzani, V.; Schmetz, J.; Lutz, H.J.; Kerkmann, J.; Alberoni, P.P.; Cervino, M. Precipitation estimations from geostationary orbit and prospects for METEOSAT Second Generation. *Meteorol. Appl.* **2001**, *8*, 23–41. [CrossRef]
- Villarini, G.; Krajewski, W.F. Review of the different sources of uncertainty in single polarization radar-based estimates of rainfall. *Surv. Geophys.* **2010**, *31*, 107–129. [CrossRef]
- Ośródk, K.; Szturc, J.; Jurczyk, A. Chain of data quality algorithms for 3-D single-polarization radar reflectivity (RADVOL-QC system). *Meteorol. Appl.* **2014**, *21*, 256–270. [CrossRef]
- Hsu, S.Y.; Chen, T.B.; Du, W.C.; Wu, J.H.; Chen, S.C. Integrate Weather Radar and Monitoring Devices for Urban Flooding Surveillance. *Sensors* **2019**, *19*, 825. [CrossRef] [PubMed]
- Rapant, P.; Kolejka, J. Dynamic Pluvial Flash Flooding Hazard Forecast Using Weather Radar Data. *Remote Sens.* **2021**, *13*, 2943. [CrossRef]

21. McCarthy, N.; Guyot, A.; Dowdy, A.; McGowan, H. Wildfire and Weather Radar: A Review. *J. Geophys. Res. Atmos.* **2019**, *124*, 266–286. [CrossRef]
22. Maki, M.; Kim, Y.; Kobori, T.; Hirano, K.; Lee, D.I.; Iguchi, M. Analyses of three-dimensional weather radar data from volcanic eruption clouds. *J. Volcanol. Geotherm. Res.* **2021**, *412*, 107178. [CrossRef]
23. Marzano, F.S.; Barbieri, S.; Vulpiani, G.; Rose, W.I. Volcanic ash cloud retrieval by ground-based microwave weather radar. *IEEE Trans. Geosci. Remote Sens.* **2006**, *44*, 3235–3245. [CrossRef]
24. Voormansik, T.; Rossi, P.J.; Moisseev, D.; Tanilsoo, T.; Post, P. Thunderstorm hail and lightning detection parameters based on dual-polarization Doppler weather radar data. *Meteorol. Appl.* **2017**, *24*, 521–530. [CrossRef]
25. Kranstauber, B.; Bouten, W.; Leijnse, H.; Wijers, B.-C.; Verlinden, L.; Shamoun-Baranes, J.; Dokter, A.M. High-Resolution Spatial Distribution of Bird Movements Estimated from a Weather Radar Network. *Remote Sens.* **2020**, *12*, 635. [CrossRef]
26. McLaren, J.D.; Buler, J.J.; Schreckengost, T.; Smolinsky, J.A.; Boone, M.; Emiel van Loon, E.; Dawson, D.K.; Walters, E.L. Artificial light at night confounds broad-scale habitat use by migrating birds. *Ecol. Lett.* **2018**, *21*, 356–364. [CrossRef]
27. Nilsson, C.; Dokter, A.M.; Verlinden, L.; Shamoun-Baranes, J.; Schmid, B.; Desmet, P.; Bauer, S.; Chapman, J.; Alves, J.A.; Stepanian, P.M.; et al. Revealing patterns of nocturnal migration using the European weather radar network. *Ecography* **2019**, *42*, 876–886. [CrossRef]
28. Rosenberg, K.V.; Dokter, A.M.; Blancher, P.J.; Sauer, J.R.; Smith, A.C.; Smith, P.A.; Stanton, J.C.; Panjabi, A.; Helft, L.; Parr, M.; et al. Decline of the North American avifauna. *Science* **2019**, *366*, 120–124. [CrossRef] [PubMed]
29. Trombe, P.-J.; Pinson, P.; Vincent, C.; Bøvith, T.; Cutululis, N.A.; Draxl, C.; Giebel, G.; Hahmann, A.N.; Jensen, N.E.; Jensen, B.P.; et al. Weather radars—The new eyes for offshore wind farms? *Wind. Energy* **2014**, *17*, 1767–1787. [CrossRef]
30. Qian, Z.; Yang, C.; Xu, H.; Cui, Y.; Han, Y.; Zhao, C.; Lv, Q. Analysis and Study on the Interference of Wind Farms to the New Generation Weather Radar Echoes. In Proceedings of the 5th International Conference on Information Science and Control Engineering (ICISCE), Zhengzhou, China, 20–22 July 2018; pp. 1086–1092. [CrossRef]
31. Zewdie, G.K.; Lary, D.J.; Liu, X.; Wu, D.; Levetin, E. Estimating the daily pollen concentration in the atmosphere using machine learning and NEXRAD weather radar data. *Environ. Monit. Assess.* **2019**, *191*, 418. [CrossRef] [PubMed]
32. Lischi, S.; Lupidi, A.; Martorella, M.; Cuccoli, F.; Facheris, L.; Baldini, L. Advanced polarimetric doppler weather radar simulator. In Proceedings of the International Radar Symposium, Gdansk, Poland, 16–18 June 2014. [CrossRef]
33. Li, Z.; Perera, S.; Zhang, Y.; Zhang, G.; Doviak, R. Phased-Array Radar System Simulator (PASIM): Development and Simulation Result Assessment. *Remote Sens.* **2019**, *11*, 422. [CrossRef]
34. Li, Z.; Zhang, Y.; Zhang, G.; Brewster, K.A. A microphysics-based simulator for advanced airborne weather radar development. *IEEE Trans. Geosci. Remote Sens.* **2011**, *49*, 1356–1373. [CrossRef]
35. Zeng, Q.; He, J.; Shi, Z.; Li, X. Weather radar data compression based on spatial and temporal prediction. *Atmosphere* **2018**, *9*, 96. [CrossRef]
36. Vaccarone, M.; Chandrasekar, C.V.; Bechini, R.; Cremonini, R. Survey on Electromagnetic Interference in Weather Radars in Northwestern Italy. *Environments* **2019**, *6*, 126. [CrossRef]
37. Oh, Y.A.; Kim, H.L.; Suk, M.K. Clutter Elimination Algorithm for Non-Precipitation Echo of Radar Data Considering Meteorological and Observational Properties in Polarimetric Measurements. *Remote Sens.* **2020**, *12*, 3790. [CrossRef]
38. Nepal, R.; Zhang, Y.; Blake, W. Sense and Avoid Airborne Radar Implementations on a Low-Cost Weather Radar Platform. *Aerospace* **2017**, *4*, 11. [CrossRef]
39. Nekrasov, A.; Khachatryan, A.; Veremyev, V.; Bogachev, M. Sea Surface Wind Measurement by Airborne Weather Radar Scanning in a Wide-Size Sector. *Atmosphere* **2016**, *7*, 72. [CrossRef]
40. Barge, B.L.; Humphries, R.G.; Mah, S.J.; Kuhnke, W.K. Rainfall measurements by weather radar: Applications to hydrology. *Water Resour. Res.* **1979**, *15*, 1380–1386. [CrossRef]
41. Seo, D.J.; Habib, E.; Andrieu, H.; Morin, E. Hydrologic applications of weather radar. *J. Hydrol.* **2015**, *531*, 231–233. [CrossRef]
42. Wijayarathne, D.; Boodoo, S.; Coulibaly, P.; Sills, D. Evaluation of Radar Quantitative Precipitation Estimates (QPEs) as an Input of Hydrological Models for Hydrometeorological Applications. *J. Hydrometeorol.* **2020**, *21*, 1847–1864. [CrossRef]
43. Chen, H.; Chandrasekar, V. The quantitative precipitation estimation system for Dallas-Fort Worth (DFW) urban remote sensing network. *J. Hydrol.* **2015**, *531*, 259–271. [CrossRef]
44. Seo, B.C.; Krajewski, W.F. Correcting temporal sampling error in radar-rainfall: Effect of advection parameters and rain storm characteristics on the correction accuracy. *J. Hydrol.* **2015**, *531*, 272–283. [CrossRef]
45. Sandford, C.; Illingworth, A.; Thompson, R. The Potential Use of the Linear Depolarization Ratio to Distinguish between Convective and Stratiform Rainfall to Improve Radar Rain-Rate Estimates. *J. Appl. Meteorol. Climatol.* **2017**, *56*, 2927–2940. [CrossRef]
46. Kwon, S.; Jung, S.H.; Lee, G.W. Inter-comparison of radar rainfall rate using Constant Altitude Plan Position Indicator and hybrid surface rainfall maps. *J. Hydrol.* **2015**, *531*, 234–247. [CrossRef]
47. Scopus—Document Details—Comparison of Radar Algorithms for Quantitative Precipitation Estimations in the Canadian Precipitation Analysis (CaPA) from Operational Polarimetric Radars for Hydrological Applications | Signed in. Available online: <https://www.scopus.com/record/display.uri?eid=2-s2.0-84964429128&origin=inward> (accessed on 29 November 2021).

48. Rafieeinassab, A.; Norouzi, A.; Kim, S.; Habibi, H.; Nazari, B.; Seo, D.-J.; Lee, H.; Cosgrove, B.; Cui, Z. Toward high-resolution flash flood prediction in large urban areas—Analysis of sensitivity to spatiotemporal resolution of rainfall input and hydrologic modeling. *J. Hydrol.* **2015**, *531*, 370–388. [CrossRef]
49. Kim, B.; Seo, D.J.; Noh, S.J.; Prat, O.P.; Nelson, B.R. Improving multisensor estimation of heavy-to-extreme precipitation via conditional bias-penalized optimal estimation. *J. Hydrol.* **2018**, *556*, 1096–1109. [CrossRef]
50. Influence of Rainfall Spatial Variability on Hydrological Modelling: Study by Simulations-Web of Science Core Collection. Available online: <https://biblioproxy.cnr.it:3009/wos/woscc/full-record/WOS:000313597100083> (accessed on 29 November 2021).
51. Quantifying Catchment-Scale Storm Motion and its Effects on Flood Response-Web of Science Core Collection. Available online: <https://biblioproxy.cnr.it:3009/wos/woscc/full-record/WOS:000313597100084> (accessed on 29 November 2021).
52. Dyer, J.L.; Garza, R.C. A comparison of precipitation estimation techniques over Lake Okeechobee, Florida. *Weather Forecast.* **2004**, *19*, 1029–1043. [CrossRef]
53. Wang, L.P.; Ochoa-Rodríguez, S.; Simões, N.E.; Onof, C.; Maksimović, Č. Radar-rain gauge data combination techniques: A revision and analysis of their suitability for urban hydrology. *Water Sci. Technol.* **2013**, *68*, 737–747. [CrossRef] [PubMed]
54. Radar-Based Pluvial Flood Forecasting over Urban Areas: Redbridge Case Study-Web of Science Core Collection. Available online: <https://biblioproxy.cnr.it:3009/wos/woscc/full-record/WOS:000313597100102> (accessed on 29 November 2021).
55. Ochoa-Rodríguez, S.; Wang, L.P.; Willems, P.; Onof, C. A Review of Radar-Rain Gauge Data Merging Methods and Their Potential for Urban Hydrological Applications. *Water Resour. Res.* **2019**, *55*, 6356–6391. [CrossRef]
56. Ochoa-Rodríguez, S.; Wang, L.-P.; Gires, A.; Pina, R.D.; Reinoso-Rondinel, R.; Bruni, G.; Ichiba, A.; Gaitan, S.; Cristiano, E.; van Assel, J.; et al. Impact of spatial and temporal resolution of rainfall inputs on urban hydrodynamic modelling outputs: A multi-catchment investigation. *J. Hydrol.* **2015**, *531*, 389–407. [CrossRef]
57. Marra, F.; Morin, E. Use of radar QPE for the derivation of Intensity-Duration-Frequency curves in a range of climatic regimes. *J. Hydrol.* **2015**, *531*, 427–440. [CrossRef]
58. Eldardiry, H.; Habib, E.; Zhang, Y.; Grascchel, J. Artifacts in Stage IV NWS Real-Time Multisensor Precipitation Estimates and Impacts on Identification of Maximum Series. *J. Hydrol. Eng.* **2017**, *22*, E4015003. [CrossRef]
59. Campos, E.; Wang, J. Numerical simulation and analysis of the April 2013 Chicago Floods. *J. Hydrol.* **2015**, *531*, 454–474. [CrossRef]
60. Wilson, A.M.; Barros, A.P. Landform controls on low level moisture convergence and the diurnal cycle of warm season orographic rainfall in the Southern Appalachians. *J. Hydrol.* **2015**, *531*, 475–493. [CrossRef]
61. Yu, F.; Zhuge, X.Y.; Zhang, C.W. Rainfall retrieval and nowcasting based on multispectral satellite images. Part II: Retrieval study on daytime half-hour rain rate. *J. Hydrometeorol.* **2011**, *12*, 1271–1285. [CrossRef]
62. Conti, F.I.; Francipane, A.; Pumo, D.; Noto, L.V. Exploring single polarization X-band weather radar potentials for local meteorological and hydrological applications. *J. Hydrol.* **2015**, *531*, 508–522. [CrossRef]
63. Kundzewicz, Z.; Kanae, S.; Seneviratne, S.; Handmer, J.; Nicholls, N.; Peduzzi, P.; Mechler, R.; Bouwer, L.M.; Arnell, N.; Mach, K.; et al. Flood risk and climate change: Global and regional perspectives. *Hydrol. Sci. J.* **2014**, *59*, 1–28. [CrossRef]
64. Khalequzzaman, M. Recent floods in Bangladesh: Possible causes and solutions. *Nat. Hazards* **1994**, *9*, 65–80. [CrossRef]
65. Amadio, M.; Scorzini, A.R.; Carisi, F.; Essenfelder, A.H.; Domeneghetti, A.; Mysiak, J.; Castellarin, A. Testing empirical and synthetic flood damage models: The case of Italy. *Nat. Hazards Earth Syst. Sci.* **2019**, *19*, 661–678. [CrossRef]
66. Alfieri, L.; Feyen, L.; Salamon, P.; Thielen, J.; Bianchi, A.; Dottori, F.; Burek, P. Modelling the socio-economic impact of river floods in Europe. *Nat. Hazards Earth Syst. Sci.* **2016**, *16*, 1401–1411. [CrossRef]
67. Pistrika, A.K.; Jonkman, S.N. Damage to residential buildings due to flooding of New Orleans after hurricane Katrina. *Nat. Hazards* **2010**, *54*, 413–434. [CrossRef]
68. Horita, F.A.; Martins, R.G.; Palma, G.; Vilela, R.B.; Bressiani, D.A.; de Albuquerque, J.P. Determining flooded areas using crowd sensing data and weather radar precipitation: A case study in Brazil. In Proceedings of the 15th International Conference on Information Systems for Crisis Response and Management, Rochester, NY, USA, 20–23 May 2018; Boersma, K., Tomaszewski, B., Eds.; Available online: <http://wrap.warwick.ac.uk/102615> (accessed on 25 November 2021).
69. Millennium Ecosystem Assessment (MA). *Ecosystems and Human Well-Being: Synthesis*; Island Press: Washington, DC, USA, 2005.
70. Cimini, D.; Romano, F.; Ricciardelli, E.; Di Paola, F.; Viggiano, M.; Marzano, F.S.; Colaiuda, V.; Picciotti, E.; Vulpiani, G.; Cuomo, V. Validation of satellite OPEMW precipitation product with ground-based weather radar and rain gauge networks. *Atmos. Meas. Tech.* **2013**, *6*, 3181–3196. [CrossRef]
71. Radar Platform | Dipartimento della Protezione Civile. Available online: <https://mappe.protezionecivile.gov.it/en/risks-maps/radar-map> (accessed on 28 November 2021).
72. Data Management and Production of the National Radar Network. 2018. Available online: <https://www.mydewetra.org/wiki/images/8/8e/ReteRadatHDF5.pdf> (accessed on 28 November 2021).
73. Massarelli, C.; Losacco, D.; Tumolo, M.; Campanale, C.; Uricchio, V.F. Protection of Water Resources from Agriculture Pollution: An Integrated Methodological Approach for the Nitrates Directive 91–676-EEC Implementation. *Int. J. Environ. Res. Public Health* **2021**, *18*, 13323. [CrossRef]
74. DTM. Available online: <http://webapps.sit.puglia.it/freewebapps/DTM/index.html> (accessed on 28 November 2021).
75. Descrizione Della Piattaforma—radar-dpc-docs 1.0 Documentazione. Available online: <https://dpc-radar.readthedocs.io/it/latest/platform.html> (accessed on 28 November 2021).

76. Accesso ai Servizi WMS e WMTS—Radar-dpc-docs 1.0 Documentazione. Available online: <https://dpc-radar.readthedocs.io/it/latest/services.html> (accessed on 28 November 2021).
77. GeoServer. Available online: <http://geoserver.org/> (accessed on 28 November 2021).
78. The Home of Location Technology Innovation and Collaboration | OGC. Available online: <https://www.ogc.org/> (accessed on 28 November 2021).
79. Laender, A.H.F.; Ribeiro-Neto, B.A.; da Silva, A.S.; Teixeira, J.S. A brief survey of web data extraction tools. *ACM SIGMOD Rec.* **2002**, *31*, 84–93. [CrossRef]
80. Welcome to Python.org. Available online: <https://www.python.org/> (accessed on 28 November 2021).
81. Welcome to the Python GDAL/OGR Cookbook!—Python GDAL/OGR Cookbook 1.0 Documentation. Available online: <http://pcjericks.github.io/py-gdalogr-cookbook/index.html#> (accessed on 28 November 2021).
82. GDAL—GDAL Documentation. Available online: <https://gdal.org/index.html> (accessed on 28 November 2021).
83. GeoWebCache. Available online: <https://radar-geowebcache.protezionecivile.it/service/wmts?REQUEST=getcapabilities> (accessed on 28 November 2021).
84. Mappa Stazioni Meteo | Agrometeopuglia—ARIF PUGLIA. Available online: <http://www.agrometeopuglia.it/osservazioni/mappa-stazioni-meteo> (accessed on 28 November 2021).
85. Meteo—Geoportale del Servizio Agenti Fisici—Lizmap. Available online: <http://www.webgis.arpa.puglia.it/lizmap/index.php/view/map/?repository=1&project=meteo> (accessed on 28 November 2021).
86. Shepard, D. A two-dimensional interpolation function for irregularly-spaced data. In Proceedings of the 23rd ACM National Conference, Las Vegas, NV, USA, 27–29 August 1968; ACM Press: New York, NY, USA, 1968; pp. 517–524. [CrossRef]
87. AGID, Agency for Digital Italy. Adoption of the "Technologies and Standards Guidelines for Interoperability Safety through the Computer Systems API "and the" Guidelines on the Technical Interoperability of the Publics Administration". Available online: <https://www.agid.gov.it/en/linee-guida> (accessed on 28 November 2021).